2018

Toward the detection of the triatomic negative ion SPN−: Spectroscopy and potential energy surfaces

Tarek Trabelsi
University of Nebraska-Lincoln, tarek.trabelsi@unl.edu

Majdi Hochlaf
Universite Paris-Est

Joseph S. Francisco
University of Nebraska-Lincoln, frjoseph@sas.upenn.edu

Toward the detection of the triatomic negative ion SPN^-: Spectroscopy and potential energy surfaces

Tarek Trabelsi,[1] Majdi Hochlaf,[2] and Joseph S. Francisco[1,a)]
[1]*Department of Chemistry, University of Nebraska-Lincoln, Lincoln, Nebraska 68588, USA*
[2]*Université Paris-Est, Laboratoire Modélisation et Simulation Multi Echelle, MSME UMR 8208 CNRS, 5 Blvd. Descartes, 77454 Marne-la-Vallée, France*

(Received 12 March 2018; accepted 10 April 2018; published online 24 April 2018)

High level theoretical calculations using coupled-cluster theory were performed to provide an accurate description of the electronic structure, spectroscopic properties, and stability of the triatomic negative ion comprising S, N, and P. The adiabatic electron affinities (AEAs) and vertical detachment energies (VDEs) of PNS, SPN, PSN, and *cyc*-PSN were calculated. The predicted AEA and VDE of the linear SPN isomer are large: 2.24 and 3.04 eV, respectively. The potential energy surfaces (PESs) of the lowest-lying electronic states of the SPN^- isomer along the PN and SP bond lengths and bond angle were mapped. A set of spectroscopic parameters for SPN^-, PNS^-, and PSN^- in their electronic ground states is obtained from the 3D PESs to help detect these species in the gas phase. The electronic excited state $SPN^-(1^2A'')$ is predicted to be stable with a long lifetime calculated to be 189.7 μs. The formation of SPN^- in its electronic ground state through the bimolecular collision between S^- + PN and N + PS^- is also discussed. *Published by AIP Publishing.* https://doi.org/10.1063/1.5029275

I. INTRODUCTION

Molecular anions are of major theoretical interest as a benchmark to develop models and basis sets. Their electronic structure, spectroscopic parameters, stability, and other chemical properties need to be characterized theoretically because experimental studies on these species are often difficult. An understanding of their formation process and their stability is of fundamental importance in describing their role in various processes.[1–5] In astrophysics, a limited number of negative ions have been detected in the interstellar medium (ISM) compared to those of neutral molecules.[6–10] Their role and their abundance in the ISM have not yet been clarified. Anion formation may occur via collisional processes[11] or via dipole-bond formation pathways.[12,13]

Although electrons are one of the most abundant species in dense molecular clouds,[14] because of this high density, a significant fraction of large molecules with sufficient electron affinities can be present in dense molecular clouds despite the increased UV flux in this region.[15,16] The discovery of several molecules containing second and third row elements in the ISM, especially phosphorus and sulfur,[17] has inspired experimentalists to synthesize new molecular species in the gas phase that may be present in the ISM, such as PNX and PCX^- (X = O, S).[18–21] These species are characterized by large electron affinities (>2 eV) and the ability to readily add electrons. The electronic structure, stability, and spectroscopic parameters of the triatomic ion of S, N, and P have been studied theoretically[22,23] and experimentally.[20] Three isomers, namely, SNP, SPN, and *cyc*-PSN, have been identified in the gas phase.[20] High accurate computations predict the existence of linear PSN, which is 2.4 eV higher in energy than the most stable linear SNP isomer.[22] However, spectroscopic data and stability of its corresponding anion and cations are still lacking.

The purpose of the present work is to fully characterize the geometrical parameters, harmonic vibrational frequencies, and rotational constants of all PNS^- species in their electronic ground states with high-level *ab initio* computations. We then deduce their stability and electron affinities. For the investigation, coupled-cluster and explicitly correlated coupled-cluster theories were chosen. In the second part of this work, the low-lying doublet and quartet electronic states of the most stable isomer SPN^- were calculated with multireference configuration interaction (MRCI) wavefunctions and a large basis set augmented by diffuse atomic functions. The potential energy surfaces (PESs) along the bending and stretching coordinates were mapped. This work represents the first theoretical investigations of the electronic structure and the spectroscopic constants of the anionic SPN species and should help with detecting these charged species in the laboratory.

II. COMPUTATIONAL DETAILS

Ab initio electronic structure calculations were performed using the MOLPRO 2015 program.[24] Restricted coupled-cluster theory with single and double excitations and a perturbative triple correction RCCSD(T)[25,26] and the explicitly correlated version RCCSD(T)-F12[27–29] were used for the evaluation of the electronic ground state, accurate equilibrium geometric parameters, rotational constant, electronic affinities, and harmonic vibrational frequencies. It is known that diffuse basis sets are required to calculate anion states. In this

a)Author to whom correspondence should be addressed: jfrancisco3@unl.edu

work, we used the augmented correlation-consistent aug-cc-pVXZ (X = D, T, Q, and 5) basis sets to describe nitrogen atoms and the basis sets containing an extra tight *d* function aug-cc-pV(X+d)Z[30,31] to describe sulfur and phosphorus atoms. These are denoted hereafter as aVXZ and aV(X+d)Z, respectively. For the explicitly correlated method CCSD(T)-F12, the basis sets[32] cc-pVnZ-F12 (n = D, T, and Q) were used. The total energies and geometrical parameters were extrapolated to the complete basis set (CBS) limit using the two-parameter equations $E_X = E_{CBS} + A/X^3$, where A is a fitting parameter.[33]

For the investigations of the electronic excited states of the most stable isomer SPN^-, we used the complete active space self-consistent field (CASSCF) method[34,35] followed by the internally contracted multireference configuration interaction (MRCI) method,[36,37] as implemented into the MOLPRO package. In these calculations, the atoms were described using a diffuse basis set of aV5Z/aV(5+d)Z quality. The CASSCF active space was defined considering all valence orbitals, whereas the 1s core orbital of nitrogen and 1s, 2s, and 2p core orbitals of sulfur and phosphorus were kept doubly occupied. All electronic states with the same spin-multiplicity were averaged together. In the MRCI calculations, we considered all configurations of the CI expansion of the CASSCF wavefunctions as a reference. From the CASSCF wavefunction, the transition dipole moment was evaluated to calculate the lifetime (τ in s), which is related to the square of the transition dipole moment ($|R_{e,i}|^2$ in D) via the following equation:

$$\tau\,(s) = 6.077\,06 \times 10^{-6} \sum_{i}^{n} \frac{1}{|R_{e,i}|^2 \delta E_i{}^3},$$

where the δE_i is the energy transition in eV and n is the number of electronic states.

The 3D PESs of SNP^-, SPN^-, and PSN^- were mapped in internal coordinates corresponding to the R_{PN}, R_{SN}, and R_{PS} bond lengths and to the in-plane bending angle θ. Calculations were conducted at several nuclear geometries around the equilibrium geometry for each isomer. Then, the calculated energies were fitted to this expansion

$$V(R_1,R_2,\theta) = \sum\nolimits_{i,j,k} C_{ijk}(R_1,R_{1eq})^i(R_2 - R_{2eq})^i(\theta - \theta_{eq})^k,$$

where R_{1eq}, R_{2eq}, and θ_{eq} refer to the equilibrium coordinates. The C_{ijk} coefficients were optimized using a least-squares procedure.

For the fit, we restricted the exponents in the expansion to $i + j + k \leq 4$. The resulting PESs were used to compute the spectroscopic constants with the SURFIT[38,39] program.

III. RESULTS AND DISCUSSION

A. Electronic structure

The optimized equilibrium geometries and harmonic vibrational frequencies of SPN^-, SNP^-, *cyc*-PSN^-, and PSN^- in their electronic ground states are listed in Table I and Table SI of the supplementary material. We also provide the equilibrium geometry of their corresponding neutral species[22] in Table SI. Examination of these tables reveals that as the size of the basis increases, the geometrical parameters converge. On the other hand, the results obtained with the explicitly correlated coupled-cluster method show faster convergence and are closer to the complete basis set values. We should note also that the RCCSD(T)-F12/CBS results are very similar to the results obtained using the RCCSD(T)/CBS method despite the strong reduction in the computational costs. There are no experimental or theoretical results for geometric parameters of anionic PNS species to compare with our current results. We consider our RCCSD(T)-F12/CBS results as the best estimate of the investigated geometrical parameters. These values will be quoted in the following discussion.

Among the neutral species,[22] the most stable isomer is linear SNP, which has $C_{\infty v}$ symmetry and $X^1\Sigma^+$ electronic ground state. Addition of an electron to form $[P,N,S]^-$ leads to four bent open-shell isomers (i.e., C_s point group): $SNP^-(X^2A')$, $SPN^-(X^2A')$, and $PSN^-(X^2A')$ and one cyclic isomer *cyc*-$PSN^-(X^2A')$. The most stable isomer is bent SPN^- with a PS bond distance of 2.012 Å and a PN bond distance of 1.545 Å. Relative to neutral SPN, SPN^- with an additional electron has an increase in the SP bond length of 0.12 Å, a similar PN bond length, whereas we observe a decrease in the SPN bond angle from 180° to 127.5°. The addition of an electron increases the electronic density localized in the PS bond region. For the SNP^- isomer, the addition of an electron slightly increases the SN bond length by 0.068 Å and the SN bond length by 0.034 Å and decreases the SNP angle from 180° to 155.9°. Similarly, the addition of one electron to PSN to form PSN^- leads to a substantial change in the geometry: the SP distance increases significantly by 0.110 Å, and the SN distance increases by 0.040 Å. Note that relative to those in *cyc*-PSN, the SN and PS bond lengths in *cyc*-PSN^- have decreased by 0.081 Å and 0.056 Å. These changes in the equilibrium geometries of these species should have an effect on their stability and spectroscopic parameters.

All SNP^- species present a real minimum in their ground state PES since all their corresponding frequencies are positive (see Table I and Table SI of the supplementary material). For SPN^-, at the RCCSD(T)/aV(5+d)Z level of theory, we compute PN and SP harmonic frequencies of 1084.2 and 535.1 cm^{-1}, respectively. A bending frequency of 203.5 cm^{-1} is computed. For SNP^-, we compute PN and SN stretching frequencies of 1220.5 and 582.5 cm^{-1}, respectively, and a bending frequency of 189.1 cm^{-1} at the same level. Furthermore, we obtained ω_1 (SN stretch) = 1056.7, ω_2 (bend) = 308.5, and ω_3 (SP stretch) = 509 cm^{-1} for PSN^- and ω_1 (PN stretch) = 890.6, ω_2 (asymmetric ring) = 426.8, and ω_3 (symmetric ring) = 533.1 cm^{-1} for *cyc*-PSN^-. Adding an electron to a neutral species leads to a large change in its harmonic vibrational frequencies. As can be seen in Table I, the PN and SP stretching frequencies in the SPN^- isomer are decreased by 247.1 and 109.8 cm^{-1} upon attaching an electron to the neutral species. Interestingly, all isomers exhibit different sets of vibrational frequencies, which may help with their identification in mixtures. Hence, both SPN^- and SNP^- isomers have bending modes with a frequency of ~200 cm^{-1} that can be probed using far-IR

TABLE I. Optimized equilibrium geometry (R_{PN}, R_{SN}, and R_{PS} in angstroms and θ in degrees), harmonic vibrational frequencies (ω_i in cm^{-1}), total energy (in hartree), and relative energies (E_r in eV) of SPN^-, SNP^-, *cyc*-PSN^-, and PSN^- computed at different levels of theory.

				$SPN^-(X^2A')$					
	Basis	R_{SP}	R_{PN}	θ	ω_1	ω_2	ω_3	Energy	Er
CCSD(T)	aV(5+d)Z	2.014	1.547	127.2	1084.2	203.5	535.1	−793.411 695 7	0.00
	CBS	2.013	1.546	127.2				−793.417 180 5	0.00
CCSD(T)-F12	VQZ-F12	2.012	1.545	127.5	1091.3	204.9	535.7	−793.417 971 8	0.00
	CBS	2.012	1.545	127.5				−793.421 572 0	0.00
				$SNP^-(X^2A')$					
	Basis	R_{SN}	R_{PN}	θ	ω_1	ω_2	ω_3	Energy	Er
CCSD(T)	aV(5+d)Z	1.630	1.561	155.8	1220.5	189.1	582.5	−793.380 621 8	0.84
	CBS	1.629	1.560	155.9				−793.385 804 3	0.85
CCSD(T)-F12	VQZ-F12	1.629	1.560	155.6	1221.1	193.5	585.3	−793.386 391 3	0.85
	CBS	1.629	1.559	155.8				−793.389 834 6	0.86
				cyc-$PSN^-(X^2A')$					
	Basis	R_{SN}	R_{PS}	θ	ω_1	ω_2	ω_3	Energy	Er
CCSD(T)	aV(5+d)Z	1.842	2.126	48.8	890.6	426.8	533.1	−793.366 376 4	1.23
	CBS	1.841	2.124	48.8				−793.371 890 1	1.23
CCSD(T)-F12	VQZ-F12	1.839	2.123	48.8	891.9	430.6	534.7	−793.372 325 8	1.23
	CBS	1.839	2.122	48.8				−793.375 790 9	1.24
				$PSN^-(X^2A')$					
	Basis	R_{SP}	R_{SN}	θ	ω_1	ω_2	ω_3	Energy	Er
CCSD(T)	aV(5+d)Z	1.999	1.520	138.1	1056.7	308.5	509.0	−793.335 571 2	2.07
	CBS	1.997	1.519	138.1				−793.341 130 9	2.07
CCSD(T)-F12	VQZ-F12	1.997	1.518	138.1	1061.3	310.0	511.0	−793.341 615 4	2.07
	CBS	1.996	1.518	138.1				−793.345 032 8	2.08

sources either in the laboratory or at synchrotron radiation sources.

From the 3D PESs, a set of spectroscopic parameters was obtained for $SNP^-(X^2A')$, $SPN^-(X^2A')$, and $PSN^-(X^2A')$, including rotational constants, fundamental frequencies, tau constants, first-order centrifugal distortion constants, and anharmonic vibrational constants. The results are listed in Table II. From this table, the ν_1 and ν_3 fundamentals are associated with the P—N and S—N stretching modes for SNP^- and the P—N and S—P elongations for SPN^-. The ν_2 fundamental corresponds to the bending mode. This table shows the effect of the anharmonic corrections X_{ij} on the harmonic wavenumbers. At the RCCSD(T)/aV(5+d)Z level, the ν_3 stretching mode in the SNP^- isomer deviates by 15 cm^{-1} from the harmonic vibrational frequencies of SNP. Inspection of the fundamental frequencies in Table II shows that the rovibrational spectra of these species are further complicated because of the existence of anharmonic resonances (e.g., the Darling-Dennison and Fermi resonances[40]). For instance, anharmonic resonance of the type $2\nu_3 \approx \nu_1$ is expected for all isomers. Only variationally computed vibrational frequencies are reliable and comparable to experimental spectra.

B. Electron affinities and stability

A major goal of this study is to determine the electron affinity of all PNS species. None of these species have measurements or computational estimates of such quantity. The basis set plays an important role in the accuracy of the calculated electron affinities. Table III and Table SII of the supplementary material list the adiabatic electron affinities (AEAs), the vertical detachment energy (VDE), and the vertical electron affinities (VEAs) of all PNS species calculated at several levels of theory. AEA is calculated as the energy difference between the neutral species and the anion taken at their respective equilibrium geometries and corrected for the zero point vibrational energies. VDE is evaluated as the energy difference (at the equilibrium geometry of the anion) between the neutral species and the negative ion, and VEA is assessed as the energy difference (at the equilibrium geometry of the neutral species) between the neutral species and the negative ion. From this table, we can see that AEAs and VDEs converge as the size of the basis set increases. At the CCSD(T)/aV(5+d)Z level, the AEAs of SPN and PSN are calculated to be 2.24 and 1.86 eV, respectively, and their VDEs are calculated to be 3.04 and 2.41 eV, respectively. Therefore, these species

TABLE II. CCSD(T)/aV(5+d)Z rotational constants, fundamental frequencies, tau constants, first-order centrifugal distortion constants, and anharmonic vibrational constants for SNP^-, PSN^-, and SPN^- in their electronic ground state X^2A'.

	$^{32}S^{14}NP^-$	$P^{32}S^{14}N^-$	$^{32}SP^{14}N^-$
A_0 (MHz)	353 867	81 458	52 834
B_0 (MHz)	3 305	4 217	4 366
C_0 (MHz)	3 273	4 009	4 032
ν_1 (cm^{-1})	1 214.2	1 030.0	1 073.5
ν_2 (cm^{-1})	195.9	302.8	199.2
ν_3 (cm^{-1})	597.8	491.6	523.8
10^3 Dj (MHz)	0.81	1.46	2.42
D_{JK} (MHz)	−2.217 99	−0.106 0	−0.184 4
D_K (MHz)	4 369.14	18.987 6	10.290 8
R_5 (MHz)	0.092 78	0.007 3	0.013 24
χ_{11} (cm^{-1})	4.345 280	−10.536 89	−9.702 897
χ_{12} (cm^{-1})	32.827 39	−1.801 380	−2.846 431
χ_{13} (cm^{-1})	64.502 85	11.213 87	21.008 65
χ_{22} (cm^{-1})	−9.891 521	−0.502 896	−0.754 665
χ_{23} (cm^{-1})	15.175 17	−6.001 017	−3.693 926
χ_{33} (cm^{-1})	−13.674 39	−14.288 63	−11.848 66
τ_{AAAA} (MHz)	−17 467.69	−75.532 19	−40.435 47
τ_{BBBB} (MHz)	−0.003 69	−0.007 14	−0.014 09
τ_{CCCC} (MHz)	−0.002 79	−0.004 68	−0.005 91
τ_{AABB} (MHz)	5.283 32	0.366 07	0.575 34
τ_{BBCC} (MHz)	−0.003 17	−0.005 57	−0.008 67
τ_{CCAA} (MHz)	3.690 72	0.147 90	0.255 25
τ_{ABAB} (MHz)	−0.054 27	−0.050 64	−0.056 17
ζ_{12}	0.952 765	0.392 287	0.411 922
ζ_{13}	0.267 482	0.320 016	0.313 727
ζ_{23}	0.143 843	0.862 380	0.855 508
Darling-Dennison (cm^{-1})	−4.332 24	−4.084 83	−1.913 839

should readily add electrons relative to *cyc*-PSN, which has a moderate AEA. The SNP isomer is predicted to barely bind an electron with an AEA of 0.75 eV. The minimum energy needed to build SPN^- from the corresponding neutral molecule SPN in its ground state is predicted to be 1.15 eV. Dominant electron configurations of the neutral and anionic species in their electronic ground states calculated at the equilibrium geometry of the neutral species are shown in Table SIII of the supplementary material. This table shows that the anionic ground states are obtained after adding an extra electron to the (12σ) or (16a′) molecular orbitals.

With the finite field procedure as implemented in MOLPRO, the dipole moments of neutral SPN and PNS were calculated to be 2.22 and 1.55 D, respectively. For linear PSN and cyc-PSN, we computed dipole moments of 2.42 and 2.43 D, respectively, at the CCSD(T)-F12/cc-pVQZ-F12 level of theory. Since these values are relatively large, these species can have *a priori* dipole-bound states, except linear PNS, which has a dipole moment less than 2 D.

To obtain a good understanding of the stability of the SNP^-, PSN^-, SPN^-, and *cyc*-PSN^- isomers, geometry optimizations and energy calculations were performed for (i) these anionic species and their corresponding neutral molecules (i.e., SNP, PSN, SPN, and *cyc*-PSN), and (ii) the lowest dissociation limits of $SNP^{-1,0}$/$SPN^{-1,0}$ using the (R)CCSD(T)/aug-cc-pV(5+d)Z level of theory. Figure 1 displays the energy diagrams of the neutral and anionic isomers in their

TABLE III. Vertical detachment energies (VDEs), adiabatic electron affinities (AEAs), and vertical electron affinities (VEAs) of the SNP, SPN, *cyc*-SPN, and PSN isomers computed at different levels of theory. For (R)CCSD(T) computations, we used the aVXZ and aV(X+d)Z basis sets for N and P/S, respectively. For (R)CCSD(T)-F12 computations, we used the cc-pVXZ-F12 basis sets.

Species	Method	X	VDE (eV)	AEA (eV)	VEA (eV)
SNP	(R)CCSD(T)	5	1.07	0.75	0.60
		CBS	1.07		0.60
	(R)CCSD(T)-F12	Q	1.07	0.74	0.60
		CBS	1.07		0.60
SPN	(R)CCSD(T)	5	3.04	2.24	1.15
		CBS	3.04		1.15
	(R)CCSD(T)-F12	Q	3.03	2.24	0.89
		CBS	3.03		1.10
cyc-SPN	(R)CCSD(T)	5	1.32	1.21	1.04
		CBS	1.31		1.04
	(R)CCSD(T)-F12	Q	1.31	1.20	1.12
		CBS	1.31		1.15
PSN	(R)CCSD(T)	5	2.41	1.89	0.44
		CBS	2.41		0.38
	(R)CCSD(T)-F12	Q	2.41	1.88	0.28
		CBS	2.42		0.29

electronic ground states and their lowest dissociation limits. This diagram is constructed using the electron affinities of P, S,[41] PN,[42] SN,[43] and PS[44] species. We used the optimized equilibrium geometries calculated at the CCSD(T)/aug-cc-pV(5+d)Z level from Ref. 22. In this diagram, the reference energy is the energy of the $S(^1D)$ + $PN(X^1\Sigma^+)$ asymptote. For the neutral species, the $X^1\Sigma^+$ electronic ground state of SNP, which is the most stable isomer, is 0.56 lower in energy than SPN and 1.11 eV lower in energy than the *cyc*-PSN isomer. The addition of an electron to these species, however, does not conserve this order of stability: SPN^- becomes more stable than SNP^-. As seen in Fig. 1, SPN^- is 1.06 eV lower in energy than SNP^- and 1.33 eV lower in energy than *cyc*-PSN^-. Note that PSN neutral and anionic species are higher in energy, respectively. For the SPN^- and PNS^- anions, larger number of

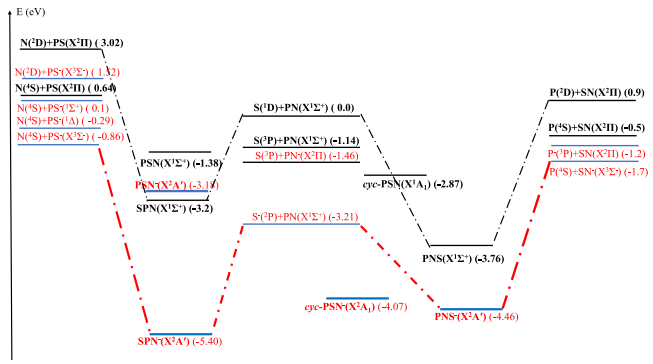

FIG. 1. Energetic diagram of the lowest bound dissociation limits for the $[P,N,S]^{-1,0}$ systems. The reference energy is the energy of the $S(^1D)$ + $PN(X^1\Sigma^+)$ asymptote.

electronic states correlating, adiabatically at large internuclear separations, to the $S/S^- + PN^-/PN$ type of fragmentation will be greater than those in $N/N^- + PS^-/PS$ and $P/P^- + SN^-/SN$. Also, this figure shows the existence of numerous anionic dissociation limits lying below their corresponding neutral dissociation limits. These potential asymptotes are important to discuss when considering the bimolecular collisions between the corresponding fragments, at least at low collision energies.

C. Calculations and representation of the potential energy surfaces

The calculations of the PESs along the PN and SP bond lengths started from the optimized equilibrium geometry at RCCSD(T)-F12/CBS. As shown in Fig. 1, the SPN^- isomer has many asymptotes that lie below those of the corresponding neutral species, and the large electron affinities of [S,P,N] system indicate that it should readily add an electron. Hence, apart from the stable electronic ground state of SPN^-, bound electronic excited states *a priori* exist in the molecular region and at large intermolecular distances. Figure 2 displays the one-dimensional cuts of the 3D PESs of the SPN/SPN^- isomers along the SP bond length [Fig. 2(a)] and along the PN bond length [Fig. 2(b)]. The evolution along the bending angle is shown in Fig. 3. Also, we present in these figures the electronic ground state of neutral SPN and the first excited state, which correlates to the lowest asymptote. In these figures, only the bound parts of the PESs are presented since the employed theoretical treatment is not adapted to study the evolution of the anionic states above the corresponding neutral parent state.

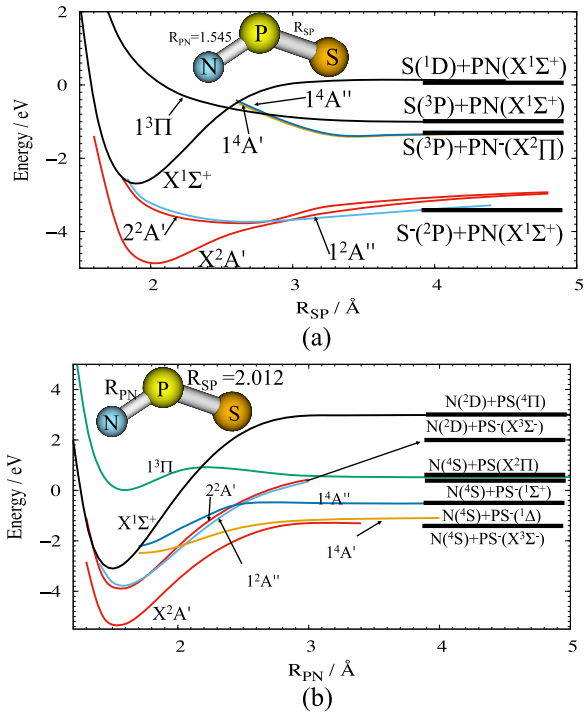

FIG. 2. MRCI/aug-cc-pV(5+d)Z one-dimensional cuts of the lowest electronic state of SPN/SPN^- along the SP bond length (a) and along the PN bond length (b). The remaining coordinates were kept fixed at their equilibrium values. The reference energy is the energy of the S(^{1}D) + PN($X^1\Sigma^+$) asymptote. The neutral potentials are in black.

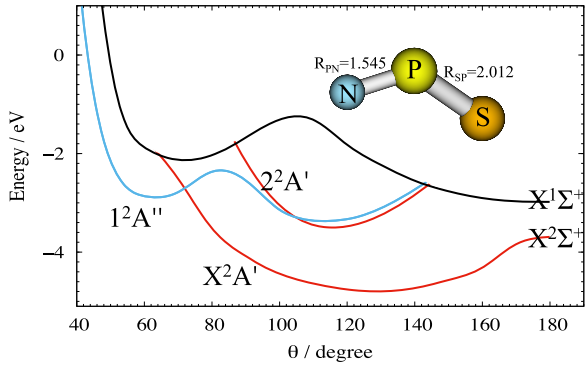

FIG. 3. MRCI/aug-cc-pV(5+d)Z one-dimensional cuts of the lowest electronic state of SPN/SPN^- along the bending angle θ. The remaining coordinates were kept fixed at their equilibrium values. The reference energy is the energy of the S(^{1}D) + PN($X^1\Sigma^+$) asymptote. The neutral potential is in black.

The reference energy is the energy of the S(^{1}D) + PN($X^1\Sigma^+$) asymptote. Figure 2(a) shows that the NPS^- (X^2A', $2^2A'$, and $1^2A''$) states correlate adiabatically to the first asymptote, $S^-(^2P)$ + PN($X^1\Sigma^+$), at large SP distances. Both the $2^2A'$ and $1^2A''$ electronic states exhibit weak potential wells. As seen in Table SIII of the supplementary material, these two electronic states are obtained after the promotion of an electron from the outermost 12σ molecular orbital (MO) into the vacant 5π or 13σ MOs. The other electronic states that correlate to S(^{3}P) + $PN^-(X^2\Pi)$, however, either have a very shallow potential due to the dipole effect (electrostatic interaction) at large intermolecular distances or are repulsive in nature. For the evolution of the doublet and quartet anionic states along the PN bond length, Fig. 2(b) shows that the $2^2A'$ and the $1^2A''$ electronic states have rather deep potential wells and correlate to N(^{2}D) + $PS^-(X^3\Sigma^-)$. At the MRCI/aV(5+d)Z level, the $1^2A''$ electronic state has PN and SP bond lengths of 1.515 Å and 2.581 Å, respectively, and the bond angle is calculated as 116.5°. This electronic state presents a real minimum in its PES since the corresponding calculated harmonic vibrational frequencies are positive: the ω_1 (PN stretch), ω_2 (bend), and ω_3 (SP stretch) are predicted to be 1 288 188, and 382 cm^{-1}, respectively. Close examination of this figure and Fig. 3 shows that the $1^2A''$ electronic state is stable. Indeed, it has a potential well located below the first dissociation limit and below its corresponding neutral ground state. Hence, the rovibrational levels of this electronic state are bound. Because of the flatness of the PES of this electronic state, large amplitude motions are expected.

The number of strongly bound electrons for SPN^- is rather limited, and electronic excitation above 3 eV leads to fast electron loss. The $2^2A'$ electronic state may be populated after Vis photon absorption, and the vertical excitation energy and the transition dipole moment from the ground state to $2^2A'$ were calculated to be 1.5 eV and 0.71 D, respectively. After Vis photon absorption, the wavepacket will explore the flat potential of $2^2A'$, subsequently producing, after dissociation, S^- + PN in their electronic ground state. Note that the transition dipole moment from the ground state to $1^2A''$ was calculated to be 0.08 D, which is relatively small compared to that computed for the ground state to $2^2A'$ transition.

At low energy collision, the formation of $SPN^-(X^2A')$ through the collision between $S^-(^2P)$ and $PN(X^1\Sigma^+)$ or $N(^4S)$ and $PS^-(X^3\Sigma^-)$ is plausible. For instance, the PES along the SP bond length suggests that the collision between S^- and PN may lead to $SPN^-(1^2A'')$. The $1^2A''$ electronic states will be significantly populated, and the subsequent transition back to the electronic ground state is accompanied by a release of energy and/or radiative emission. Note that the lifetime of this state was calculated to be 189.7 μs. Another plausible mechanism for the formation of $SPN^-(X^2A')$ is through the quartet electronic states $1^4A'$ and $1^4A''$. Figure 2(b) shows that these two quartet states, which correlate to $N(^4S) + PS^-(X^3\Sigma^-)$ and $N(^4S) + PS^-(^1\Delta)$, are crossed by the doublet states $2^2A'$ and $1^2A''$ at R_{PN} = 2.0 Å and R_{PN} = 2.4 Å, respectively. The collision between N and PS^- leads to the $1^4A'$ or $1^4A''$ electronic states, which may subsequently convert to $SPN^-(2^2A')$ or $SPN^-(2^2A'')$ after spin-orbit coupling, after the excess energy is absorbed by a third body or after radiative emission. The calculated spin-orbit matrix elements at the crossing points are relatively large, making this process reliable. Indeed, we calculate $\langle 1^4A'|H_{SO}|^2A''\rangle$ = 42.9 cm^{-1} and $\langle 1^4A'|H_{SO}|2^2A'\rangle$ = 4.09 cm^{-1} at R_{PN} = 2.0 Å. At R_{PN} = 2.4 Å, we evaluate $\langle 1^4A''|H_{SO}|2^2A'\rangle$ = 24.04 cm^{-1} and $\langle 1^4A''|H_{SO}|1^2A''\rangle$ = 28.3 cm^{-1}. The two suggestions discussed above may constitute a marker for the possible detection of SPN^- as an intermediate in reactions involving S/S^-, PS/PS^-, and PN/PN^-. The excited electronic state $1^2A''$ plays an important role in the formation of the diatomic PN. Indeed, through its flat and shallow potential, the reaction $SP^- + N = S^- + PN$ can occur and this latter may be the reason to explain the origin of PN in the interstellar medium.

IV. CONCLUSION

Electronic structure and spectroscopic parameters of PNS^-, SPN^-, PSN^-, and *cyc*-PSN^- were evaluated using coupled cluster and explicitly correlated coupled cluster theories. Our work predicts that bent SPN^- is the most stable isomer with large dipole moment and adiabatic electron affinity. The potential energy surfaces of the low-lying electronic state of SPN^- along the PN and SP bond lengths and bond angle suggest that the formation of SPN^- can occur through the bimolecular collisions between S^- and PN or between PS^- and N. The electronic excited state $1^2A''$ is predicted to be long-lived. The reaction $SP^- + N = PN + S^-$ can occur along the PES of this state. We also found favourable reaction pathways between electronic excited SN^- and P and PN^- + S, which lead mainly to the formation of the corresponding neutral triatomics $+e^-$. These reduce the possibility to detect these diatomic anions in astrophysical media. However, the anions may be viewed as intermediates during the reactions forming the neutral diatomics (PN, PS, and SN) there. The stable forms of the triatomic anions we identified here are more probable to be present in these media.

SUPPLEMENTARY MATERIAL

See supplementary material for full lists of the electronic structure computation results and for the dominant electron configurations of the species under consideration in the present study.

ACKNOWLEDGMENTS

This work is performed utilizing the Holland Computing Center of the University of Nebraska, which receives support from the Nebraska Research initiative.

[1] P. Yzombard, M. Hamamda, S. Gerber, M. Doser, and D. Comparat, Phys. Rev. Lett. **114**, 213001 (2015).
[2] D. S. Jin and J. Ye, Chem. Rev. **112**, 4801 (2012).
[3] K. Sekimoto and M. Takayama, J. Mass Spectrom. **46**, 50 (2011).
[4] T. McAllister, A. J. C. Nicholson, and D. L. Swingler, Int. J. Mass. Spectrom. Ion Phys. **27**, 43 (1978).
[5] M. Haranczyk, M. Gutowski, X. Li, and K. H. Bowen, Proc. Natl. Acad. Sci. U. S. A. **104**, 4804 (2007).
[6] S. Brünken, H. Gupta, C. A. Gottlieb, M. C. McCarthy, and P. Thaddeus, Astrophys. J. **664**, L43 (2007).
[7] J. Cernicharo, M. Guèlin, M. Agùndez, K. Kawaguchi, M. McCarthy, and P. Thaddeus, Astron. Astrophys. **467**, L37 (2007).
[8] J. Cernicharo, M. Guèlin, M. Agundez, M. C. McCarthy, and P. Thaddeus, Astrophys. J. **688**, L83 (2008).
[9] M. Agùndez, J. Cernicharo, M. Guèlin, C. Kahane, E. Roueff, J. Klos, F. J. Aoiz, F. Lique, N. Marcelino, J. R. Goicoechea, M. Gonzàlez Garcia, C. A. Gottlieb, M. C. McCarthy, and P. Thaddeus, Astron. Astrophys. **517**, L2 (2010).
[10] T. J. Millar, C. Walsh, and T. A. Field, Chem. Rev. **117**, 1765 (2017).
[11] F. Carelli, F. A. Gianturco, R. Wester, and M. Satta, J. Chem. Phys. **141**, 054302 (2014).
[12] T. Trabelsi, Y. Ajili, S. Ben Yaghlane, N.-E. Jaidane, M. Mogren Al-Mogren, J. S. Francisco, and M. Hochlaf, J. Chem. Phys. **143**, 034303 (2015).
[13] E. Herbst, Nature **289**, 656 (1981).
[14] T. J. Millar, P. R. A. Farquhar, and K. Willacy, Astron. Astrophys., Suppl. Ser. **121**, 139 (1997).
[15] S. Lepp and A. Dalgarno, Astrophys. J. **335**, 769 (1988).
[16] S. Lepp and A. Dalgarno, Astrophys. J. **324**, 553 (1988).
[17] See http://www.astro.uni-koeln.de/cdms/molecules for the list of molecules identified in the interstellar medium and circumstellar envelopes.
[18] B. Finney, A. O. Mitrushchenkov, J. S. Francisco, and K. A. Peterson, J. Chem. Phys. **145**, 224303 (2016).
[19] G.-L. Hou, B. Chen, W. J. Transue, Z. Yang, H. Grützmacher, M. Driess, C. C. Cummins, W. T. Borden, and X.-B. Wang, J. Am. Chem. Soc. **139**, 8922 (2017).
[20] X. Zeng, H. Beckers, H. Willner, and J. S. Francisco, Angew. Chem., Int. Ed. **51**, 3334 (2012).
[21] X. Q. Zeng, H. Beckers, and H. Willner, J. Am. Chem. Soc. **133**, 20696 (2011).
[22] T. Trabelsi, M. M. Al Mogren, M. Hochlaf, and J. S. Francisco, J. Chem. Phys. **148**, 054305 (2018).
[23] W. E. Turner, J. Agarwal, and H. F. Schaefer III, J. Phys. Chem. A **119**, 11693 (2015).
[24] H.-J. Werner, P. J. Knowles, G. Knizia, F. R. Manby, M. Schütz, P. Celani, T. Korona, R. Lindh, A. Mitrushenkov, G. Rauhut, K. R. Shamasundar, T. B. Adler, R. D. Amos, A. Bernhardsson, A. Berning, D. L. Cooper, M. J. O. Deegan, A. J. Dobbyn, F. Eckert, E. Goll, C. Hampel, A. Hesselmann, G. Hetzer, T. Hrenar, G. Jansen, C. Köppl, Y. Liu, A. W. Lloyd, R. A. Mata, A. J. May, S. J. McNicholas, W. Meyer, M. E. Mura, A. Nicklass, D. P. O'Neill, P. Palmieri, D. Peng, K. Pflüger, R. Pitzer, M. Reiher, T. Shiozaki, H. Stoll, A. J. Stone, R. Tarroni, T. Thorsteinsson, and M. Wang, MOLPRO, version 2015.1, a package of *ab initio* programs, 2015, see http://www.molpro.net.
[25] P. J. Knowles, C. Hampel, and H.-J. Werner, J. Chem. Phys. **99**, 5219 (1993).
[26] P. J. Knowles, C. Hampel, and H.-J. Werner, J. Chem. Phys. **112**, 3106 (2000).
[27] H. J. Werner, T. B. Adler, and F. R. Manby, J. Chem. Phys. **126**, 164102 (2007).
[28] T. B. Adler, G. Knizia, and H.-J. Werner, J. Chem. Phys. **127**, 221106 (2007).
[29] G. Knizia, T. B. Adler, and H.-J. Werner, J. Chem. Phys. **130**, 054104 (2009).
[30] D. E. Woon and T. H. Dunning, Jr., J. Chem. Phys. **98**, 1358 (1993).
[31] T. H. Dunning, Jr., K. A. Peterson, and A. K. Wilson, J. Chem. Phys. **114**, 9244 (2001).

[32]K. A. Peterson, T. B. Adler, and H.-J. Werner, J. Chem. Phys. **128**, 84102 (2008).
[33]T. Helgaker, W. Klopper, H. Koch, and J. Noga, J. Chem. Phys. **106**, 9639 (1997).
[34]P. J. Knowles and H.-J. Werner, Chem. Phys. Lett. **115**, 259 (1985).
[35]H.-J. Werner and P. J. Knowles, J. Chem. Phys. **82**, 5053 (1985).
[36]H.-J. Werner and P. J. Knowles, J. Chem. Phys. **89**, 5803 (1988).
[37]P. J. Knowles and H.-J. Werner, Chem. Phys. Lett. **145**, 514 (1988).
[38]J. Senekowitsch, "SURFIT," Ph.D. thesis, University of Frankfurt, Germany, 1988.
[39]I. M. Mills, in *Molecular Spectroscopy: Modern Research*, edited by K. N. Rao and C. W. Mathews (Academic, 1972).
[40]G. Herzberg, *Electronic Spectra and Electronic Structure of Polyatomic Molecules* (Van Nostrand, Toronto, ON, 1966).
[41]See http://webbook.nist.gov/chemistry for energy levels of atom.
[42]A. E. Kemeny, J. S. Francisco, D. A. Dixon, and D. Feller, J. Chem. Phys. **118**, 8290 (2003).
[43]S. B. Yaghlane, S. Lahmar, Z. B. Lakhdhar, and M. Hochlaf, J. Phys. B: At., Mol. Opt. Phys. **38**, 3395 (2005).
[44]S. B. Yaghlane, J. S. Francisco, and M. Hochlaf, J. Chem. Phys. **136**, 244309 (2012).